

# AUS Repository

## Stability analysis of charged neutron stars and Darmois junction conditions

Item Type	Article;Peer-Reviewed;Published version
Authors	Gul, M. Zeeshan;Sharif, M.;Arooj, Adeeba;Jami, A. Rehman;Dayanandan, Baiju
Citation	Gul, M. Z., Sharif, M., Arooj, A., Jami, A. R., & Dayanandan, B. (2024). Stability analysis of charged neutron stars and Darmois junction conditions. The European Physical Journal C, 84(8). <a href="https://doi.org/10.1140/epjc/s10052-024-13156-z">https://doi.org/10.1140/epjc/s10052-024-13156-z</a>
DOI	<a href="https://doi.org/10.1140/epjc/s10052-024-13156-z">10.1140/epjc/s10052-024-13156-z</a>
Publisher	Springer
Rights	Attribution 4.0 International
Download date	2026-03-08 23:44:49
Item License	<a href="http://creativecommons.org/licenses/by/4.0/">http://creativecommons.org/licenses/by/4.0/</a>
Link to Item	<a href="https://hdl.handle.net/11073/32607">https://hdl.handle.net/11073/32607</a>



# Stability analysis of charged neutron stars and Darmois junction conditions

M. Zeeshan Gul<sup>1,a</sup>, M. Sharif<sup>1,b</sup>, Adeeba Arooj<sup>1,c</sup>, A. Rehman Jami<sup>2,d</sup>, Baiju Dayanandan<sup>3,e</sup>

<sup>1</sup> Department of Mathematics and Statistics, The University of Lahore, 1-KM Defence Road, Lahore 54000, Pakistan

<sup>2</sup> Department of Mathematics and Statistics, College of Arts and Sciences, American University of Sharjah, Sharjah, United Arab Emirates

<sup>3</sup> Natural and Medical Sciences Research Centre, University of Nizwa, Nizwa, Oman

Received: 10 June 2024 / Accepted: 21 July 2024 / Published online: 4 August 2024  
© The Author(s) 2024

**Abstract** This research article examines the impact of  $f(Q, \mathcal{T})$  theory on the geometry of charged neutron stars filled with anisotropic matter configuration. Here,  $Q$  represents non-metricity and  $\mathcal{T}$  denotes the trace of energy-momentum tensor. We use a particular functional form of this modified theory to reduce the system's complexity and derive explicit relations of the energy density and pressure components. Further, we consider viable non-singular solutions to analyze the internal structure of the charged neutron stars. The unspecified parameters in the metric coefficients are evaluated through Darmois junction conditions, which ensures consistency between interior and exterior solutions of the stellar objects. These parameters are then used to explore different physical characteristics such as the behavior of energy density, pressure components, anisotropy, energy bounds, equation of state parameter, compactness and redshift function in the interior of charged neutron stars. The stability and equilibrium states of the charged stellar objects are discussed using the Tolman–Oppenheimer–Volkoff equation and the speed of sound, respectively. Our results suggest that the charged neutron stars are viable and stable in the presence of dark source terms.

## 1 Introduction

Modified theories of gravity are alternative approaches to address the unresolved problems in cosmology model and general relativity (GR). These theories aim to provide deeper

insights or entirely new explanations for phenomena like dark matter, dark energy, accelerating expansion of the universe and other cosmological/astrophysical observations that challenge the current understanding of the universe. Einstein's gravitational theory uses the mathematical framework of Riemannian geometry (RG), which focuses on how shapes (like spheres, curves) and distances are preserved under smooth transformations. A pivotal element in RG is the Levi-Civita connection which facilitate comparison and parallel transport of vectors while preserving their length. Weyl [1] proposed a generalization of RG to include a gauge symmetry that modifies the metric tensor at each point in spacetime. He introduced length connection which aimed to adjust vector's length during parallel transport, addressing the concept of non-metricity [2] where the covariant divergence of the metric tensor exist.

Teleparallel gravity is a framework that replace the curvature of spacetime with torsion. Here, torsion describes how vectors twist around each other in a manner that differs from curvature which describes how paths bend towards each other. This theory uses the Weitzenböck connection, which has no curvature but only torsion. In Teleparallel gravity, torsion is the fundamental quantity that represent gravitational effect. Torsion refers to the twisting of spacetime geometry as opposed to bend or curve. Despite their different approaches, Teleparallel gravity is mathematically equivalent to GR in many respects but offer a different perspective in the underlying physics. It provides the same classical test of gravity (like bending of light, perihelion precession of Mercury and gravitational time dilation) as GR. In Teleparallel gravity motion of free-falling bodies is described not by geodesics of the spacetime geometry as in GR but by force equations due to torsion tensor. In Teleparallel gravity theory, torsion serves as a tool to describe the gravitational interaction rather than curvature. Symmetric Teleparallel Gravity development and

<sup>a</sup> e-mail: [mzeeshangul.math@gmail.com](mailto:mzeeshangul.math@gmail.com) (corresponding author)

<sup>b</sup> e-mail: [msharif.math@pu.edu.pk](mailto:msharif.math@pu.edu.pk)

<sup>c</sup> e-mail: [aarooj933@gmail.com](mailto:aarooj933@gmail.com)

<sup>d</sup> e-mails: [ajami@aus.edu](mailto:ajami@aus.edu); [ajami@aus.edu](mailto:ajami@aus.edu)

<sup>e</sup> e-mail: [baiju@unizwa.edu.om](mailto:baiju@unizwa.edu.om)

exploration are active areas of research in theoretical physics, promising new insights into the fundamental forces of nature and the structure of spacetime. The action for  $f(Q)$  theory is formulated similarly to the Einstein–Hilbert action in GR, but replacing the Ricci scalar  $f(\mathcal{R})$  (which measures curvature) with a scalar  $f(Q)$  constructed from the non-metricity tensor [3]. Adak [4] discovered a spherically symmetric static solution in  $f(Q)$  gravity. Maurya et al. [5] found non-metricity parameter and decoupling constant have a significant impact on stellar objects in  $f(Q)$  gravity. Various extended theories of gravity in different context has been discussed in [6–15].

Xu and his colleagues [16,17] introduced  $f(Q, T)$  theory by including the trace of stress-energy tensor in the action of symmetric teleparallel theory. This modified proposal use connection that has neither curvature nor torsion but instead determine the concept of non-metricity to describe gravitational phenomena. Here, the presence of non-metricity quantifies how length of vectors can change under parallel transport. The primary geometric entity in this theory is non-metricity, which describes variations in the inner product of vectors transported along curves in spacetime. Thus, gravity is attributed to change in length and angles of vectors, rather than twisting or bending of spacetime. In this gravity, paths of free particles are geodesics similar to GR, but these geodesics are defined different due to absence of torsion and curvature. One of the appealing aspects of  $f(Q, T)$  theory is its applications in cosmology. The  $f(Q, T)$  theory can offer alternative explanations for dark energy and cosmic acceleration without needing additional exotic components. Researchers are motivated to study this theory for multiple reasons including its theoretical consequences and its importance in cosmic scenarios. Arora et al. [18] indicated that  $f(Q, T)$  theory addresses the late-time cosmic acceleration phenomenon. Agrawal et al. [19] studied the bouncing cosmology in this theoretical framework. Godani and Samanta [20] explored cosmic evolution using the analysis of different physical quantities in the same theory. Najera and Fajardo [21] emphasized how this modified theory offers alternatives to the standard cosmological model. Arora et al. [22] conducted a study on constraining free parameters in two distinct  $f(Q, T)$  models through energy conditions, shedding light on the viability of this theory and paving way for a new approach to understanding the dark sector of the universe. Shukla and his colleagues [23] analyzed a universe model that is both isotropic and homogeneous in this framework by studying the deceleration parameter.

Researchers are interested in understanding how the cosmic objects are formed and evolved with the passage of time. They explored various mysterious aspects of galaxies, planets, stars and claimed that these constitute a significant portions of the universe each holding its own enigmatic features. Stellar evolution and the interplay of various physical processes in star are essential topics in astrophysics. Stars are

the fundamental elements in describing structure and behavior of cosmos. Stars are big giant glowing balls of dust and gasses mainly of hydrogen and helium held together by their own gravity. The balance between gravitational collapse and energy release due to the fusion reaction is what that maintains a star's equilibrium and allows it to shine. However, stars exhaust its inner fuel to decrease its mass and pressure with increase in gravitational contraction that results in gravitational collapse of star under its own gravity. This gravitational collapse give rise to a new massive remnants known as compact star. Compact stars include white dwarfs (strong dense solid dwarf emitting light enormously), neutron stars (consist of electron and proton merge by gravity) and black holes (regions of spacetime from which nothing not even light can escape) which are incredibly dense and have small radii. Neutron stars (NSs) are further supported by the discovery of pulsars [24].

Pulsars are rotating NSs that are highly magnetized and emit beams of electromagnetic radiations [25]. They observed regular pulses of radio waves coming from a specific point in the sky and initially dubbed the source “LGM-1”. The beams of radiations emitted by pulsars are not evenly distributed but are concentrated into narrow cones that sweep across space as the NS rotates. If one of these beams happens to intersect the Earth, it is detected as a regular series of pulses at regular intervals, hence the name “pulsar”. The periods between pulses can range from milliseconds to several seconds. The period represents the time it takes for the pulsar to complete one full rotation. Pulsars emit radiations across the electromagnetic spectrum, including radio waves, X-rays and gamma rays. They are most commonly observed in radio wavelengths, where the regularity of their pulses makes them easily detectable. By studying the timing and characteristics of such pulses, astronomers can learn about their properties, such as their rotation rate, magnetic field strength and the environments in which they reside. Pulsars have been used to investigate the interstellar medium and even search for gravitational waves. Pulsars continue to be a subject of active research and new discoveries have been made regularly about these enigmatic stellar remnants. Several researchers have studied the physical attributes of NSs under various considerations [26–31].

Viable characteristics of stellar objects endorse significant progress in alternative theories. Yousaf et al. [32] used Krori–Barua metric solutions to explore some realistic configurations of anisotropic spherical structures in the background of  $f(\mathcal{R})$  gravity. Bhar et al. [33] discovered a new well-behaved charged anisotropic solution of Einstein Maxwell field equations. Zubair et al. [34] analyzed the spherically symmetric compact star model with anisotropic matter distribution admitting Finch–Skea solution satisfying the Karmarkar condition in the framework of teleparallel modified gravity. The impact of modified  $f(\mathcal{G}, T^2)$  theory on the complexity of

time-dependent dissipative as well as non-dissipative spherically symmetric celestial structures has been investigated in [35]. The spherically symmetric gravitational structure in the presence of electromagnetic field in the same theory has been studied in [36]. Yousaf [37] studied the impact of the cosmological constant on hyperbolically symmetric matter configurations. The physical characteristics of static irrotational matter content that assumes hyperbolic symmetry in  $f(\mathcal{R})$  theory has been discussed in [38]. Dayanandan [39] obtained a completely deformed Finch Skea anisotropic solution using embedding Class I spacetime. It is observed that the anisotropy enhances in the presence of gravitational decoupling, which may help in preventing the gravitational collapse of the star due to the repulsive anisotropic force. Yousaf et al. [40] analyzed the charged spherically symmetric structures through orthogonal splitting technique in the framework of  $f(\mathcal{G}, T^2)$  gravity. Khan and Yousaf [41] used the extended geometric deformation approach to explore the charged anisotropic Finch–Skea solution satisfying the Karmarkar condition. Mustafa et al. [42] studied the dynamical characteristics of an anisotropic compact star model with spherical symmetry in modified  $f(\mathcal{Q})$  theory and discovered that the compactness rises when density increases.

Yousaf [43] explored the consequences of extra curvature terms mediated from  $f(\mathcal{R}, \mathcal{T}, \mathcal{Q})$  theory on the formation of scalar functions and their importance in the study of relativistic objects. It is found that the computed one of the  $f(\mathcal{R}, \mathcal{T}, \mathcal{Q})$  structure scalars has a vital role to play in understanding celestial mechanisms in which gravitational interactions cause singularities to emerge. Khan et al. [44] explored the possibility of constructing dark matter black holes in the formalism of the Starobinsky gravity model. Yousaf et al. [45] developed black hole surrounded by fuzzy dark matter haloes, based on the Einasto density profile. They described how the coupling of the Einasto profile with an anisotropic stress energy tensor gives rise to different BH solutions corresponding to each value of the Einasto index and the rescaled mass parameter. Kunkel et al. [46] investigated non-linear structure formation in the context of fuzzy dark matter model and compared it to the cold dark matter model from a weak lensing perspective. The Fuzzy dark matter wormhole solutions coupled with anisotropic matter distribution in extended modified theories of gravity have been explored in [47]. Dome et al. [48] used high-resolution hydrodynamical N-body simulations of both cold dark matter and fuzzy dark matter cosmologies in the post-reionization redshift range. Naz et al. [49] employed the Karmarkar condition with the Finch Skea ansatz to discuss several physical properties of anisotropic compact stellar structures and explore viability as well as stability of the proposed models in  $f(\mathcal{G})$  theory. It is concluded that features of established models are in good agreement with the reality of compact stellar structures in the background of this theory. Yousaf et

al. [50] used minimal geometric deformation technique to analyze new analytical solutions that explore the influence of complexity on time-independent, spherically symmetric astrophysical configurations.

Yousaf et al. [51] examined the impact of Palatini  $f(\mathcal{R})$  terms in the formulations of inhomogeneity factors of spherical relativistic systems. Bhatti et al. [52] explored the dark dynamical effects of the  $f(\mathcal{R}, \mathcal{T})$  modified theory on the dynamics of a compact celestial star. Maurya et al. [53] used the Karmarkar condition to probe charged relativistic objects in  $f(\mathcal{G}, \mathcal{T})$  gravity. Athar et al. [54] contributed to the understanding of matter distribution and various characteristics of anisotropic CSs in the realm of  $f(\mathcal{R}, \mathcal{G})$  gravity. Bhar and Pretel [55] used metric potentials of Tolman Kuchowicz spacetime to investigate the relativistic structure of CSs in the extended symmetric teleparallel theory. Ilyas et al. [56] studied charged compact spherical structures filled with anisotropic fluid distribution in  $f(\mathcal{R}, \mathcal{G}, \mathcal{T})$  gravity. Majeed et al. [57] delved into the stability analysis of CS candidates through Tolman–Kuchvitz solutions in Rastall theory. Malik et al. [58] used the cracking technique in the same framework to assess how local density perturbations affect the stability of anisotropic stellar structures. Albalahi [59] used gravitational decoupling technique to examine the self-gravitational charged sources with spherical symmetry. Malik et al. [60] examined the static spherically symmetric structures in  $f(\mathcal{R}, \phi, \chi)$  theory. Ditta and Tiecheng [61] discussed a comprehensive analysis of the physical properties of CSs in Rastall teleparallel gravity.

Bhatti et al. [62] studied some physically viable aspects for the possible emergence of compact stars in  $f(\mathcal{G}, \mathcal{T})$  theory with some particular models. Yousaf et al. [63] investigated the possible emergence of relativistic compact stellar objects in  $f(\mathcal{R}, \mathcal{T})$  theory. Dey et al. [64] explored the viable anisotropic stellar objects employing the Finch–Skea solutions in  $f(\mathcal{R}, \mathcal{T})$  framework. Rej et al. [65] conducted a detailed examination of the charged NSs in the same theoretical framework, unveiling valuable insights into the interplay between charge and gravity in compact stellar systems. Ilyas [66] explored the viable features of strange stars in  $f(\mathcal{R}, \mathcal{G}, \mathcal{T})$  theory. Ilyas et al. [67] shed light on the intricate interplay between charge, gravity and matter in compact stellar systems. Lin and Zhai [68] investigated the influence of effective fluid parameters on the geometry of CSs in the  $f(\mathcal{Q}, \mathcal{T})$  theory. Shamir and Malik [69] provided valuable insights into the dynamical stability of compact spherical systems in modified framework. Das [70] delved into stable spherically symmetric stellar configurations in  $f(\mathcal{R}, \mathcal{G})$  gravity. Malik et al. [71] analyzed the charged anisotropic characteristics of CSs using Karmarkar condition in modified Ricci-inverse gravity.

Nashed and Capozziello [72] investigated the viable model for NSs in  $f(\mathcal{R})$  gravity, suggesting intriguing pos-

sibilities to understand the gravitational behavior of dense objects. Shamir and Rashid [73] found that the  $f(\mathcal{R})$  gravity models yield suitable and viable results with the consideration of Bardeen geometry. Ilyas and Ahmad [74] used observational data from various NS candidates to investigate the behavior of static spherical structures in the same theory. Rej and Bhar [75] employed the Durgapal-IV metric to analyze the physical characteristics of anisotropic static spherical solutions in  $f(\mathcal{R}, T)$  theory. Their examination confirmed that the obtained results remain in the physically acceptable range. Sharif et al. [10] explored the geometry of NSs with anisotropic matter configuration in modified  $f(\mathcal{R}, \phi, \chi)$  theory. Recently, the study of observational constraints in modified gravities discussed in [76–83]. The geometry of compact stars with different considerations in  $f(Q)$  and  $f(Q, T)$  theory has been studied in [84–89].

The above literatures emphasize the importance of exploring the viable attributes of charged NSs in  $f(Q, T)$  theory. This paper is formatted as follow. We employ the following pattern in this paper. In Sect. 2, we present the field equations of  $f(Q, T)$  gravity, establishing the theoretical foundation for our work. We also evaluate the unknown parameters through the Darmois junction conditions. Section 3 delves into examining different physical quantities to identify the physical characteristics exhibited by the charged NSs. Section 4 analyzes the equilibrium state and stability of the proposed NSs, providing insights into their dynamic behavior. The findings and implications of our results are given in Sect. 5.

## 2 $f(Q, T)$ theory and matching conditions

The corresponding action with matter-Lagrangian ( $\mathcal{L}_m$ ) and the Lagrangian of electromagnetic field ( $\mathcal{L}_e$ ) is expressed as [16, 17]

$$S = \frac{1}{2\kappa} \int f(Q, T) \sqrt{-g} d^4x + \int (\mathcal{L}_m + \mathcal{L}_e) \sqrt{-g} d^4x, \quad (1)$$

where Lagrangian of electromagnetic field is expressed as

$$\mathcal{L}_e = \frac{-1}{16\pi} \mathcal{F}^{\alpha\beta} \mathcal{F}_{\alpha\beta},$$

Here,  $\mathcal{F}_{\alpha\beta} = \varphi_{\alpha,\beta} - \varphi_{\beta,\alpha}$  is Maxwell field tensor and  $\varphi_\alpha$  is four-potential. The superpotential is expressed as

$$\mathcal{P}^\gamma_{\alpha\beta} = -\frac{1}{2} \mathcal{L}^\gamma_{\alpha\beta} + \frac{1}{4} (\mathcal{Q}^\gamma - \tilde{\mathcal{Q}}^\gamma) g_{\alpha\beta} - \frac{1}{4} \delta^\gamma_{[\alpha} \mathcal{Q}_{\beta]}. \quad (2)$$

The relation for non-metricity using superpotential is given by

$$\mathcal{Q} = -\mathcal{Q}_{\gamma\alpha\beta} \mathcal{P}^{\gamma\alpha\beta} = -\frac{1}{4} (-\mathcal{Q}^{\gamma\beta\eta} \mathcal{Q}_{\gamma\beta\eta}$$

$$+ 2\mathcal{Q}^{\gamma\beta\eta} \mathcal{Q}_{\eta\gamma\beta} - 2\mathcal{Q}^\eta \tilde{\mathcal{Q}}_\eta + \mathcal{Q}^\eta \mathcal{Q}_\eta). \quad (3)$$

The detailed calculation of this relation is given in [16, 17]. The resulting field equations are

$$\begin{aligned} \mathcal{T}_{\alpha\beta} + \mathcal{T}_{\alpha\beta}^E &= \frac{-2}{\sqrt{-g}} \nabla_\gamma (f_Q \sqrt{-g} \mathcal{P}^\gamma_{\alpha\beta}) \\ &- \frac{1}{2} f g_{\alpha\beta} + f_T (\mathcal{T}_{\alpha\beta} + \Theta_{\alpha\beta}) \\ &- f_Q (\mathcal{P}_{\alpha\gamma\eta} \mathcal{Q}_\beta^{\gamma\eta} - 2\mathcal{Q}^\gamma_\alpha \mathcal{P}_{\gamma\eta\beta}), \end{aligned} \quad (4)$$

where  $f_Q$  and  $f_T$  represent the derivatives corresponding to non-metricity and trace of stress-energy tensor, respectively.

To explore the structure of charged stellar objects, we consider static spherical metric as

$$ds^2 = dt^2 e^{\mu(r)} - dr^2 e^{\nu(r)} - d\theta^2 r^2 - d\phi^2 r^2 \sin^2 \theta. \quad (5)$$

The anisotropic matter distribution with four-vector ( $\mathcal{V}_\alpha$ ) and four-velocity ( $\mathcal{U}_\alpha$ ) is defined as [90]

$$\mathcal{T}_{\alpha\beta} = \mathcal{U}_\alpha \mathcal{U}_\beta \rho + P_r \mathcal{V}_\alpha \mathcal{V}_\beta - P_t g_{\alpha\beta} + P_t (\mathcal{U}_\alpha \mathcal{U}_\beta - \mathcal{V}_\alpha \mathcal{V}_\beta), \quad (6)$$

where  $\rho$ ,  $P_r$  and  $P_t$  define the energy density, radial pressure and tangential pressure of the fluid, respectively. The matter-Lagrangian is important in various cosmic phenomena as it demonstrates the configuration of fluid in spacetime. The particular value of matter-Lagrangian can yields significant insights. The well known used formulation of the matter-Lagrangian in the literature is  $\mathcal{L}_m = -\frac{P_r + 2P_t}{3}$  [91].

The Maxwell equations of motion with four-current ( $\mathcal{J}^\alpha$ ) and charge density ( $\sigma$ ) are expressed as

$$\mathcal{F}_{[\alpha\beta;\gamma]} = 0, \quad \mathcal{F}^{\alpha\beta}_{;\beta} = 4\pi \mathcal{J}^\alpha, \quad (7)$$

where

$$\mathcal{J}^\alpha = \sigma \mathcal{U}^\alpha. \quad (8)$$

The corresponding Maxwell field equation becomes

$$\varphi'' - \left( \frac{\mu'}{2} + \frac{\nu'}{2} - \frac{2}{r} \right) \varphi' = 4\pi \sigma^{\frac{\mu+\nu}{2}}, \quad (9)$$

where prime is radial derivative and  $q(r)$  is total charge in the NSs. Integrating Eq. (9) yields

$$\varphi' = \frac{q(r)}{r^2} e^{\frac{\mu+\nu}{2}}, \quad q(r) = 4\pi \int_0^r \sigma r^2 e^{\frac{\mu}{2}} dr, \quad E = \frac{q}{4\pi r^2}.$$

The modified field equations for static spherical spacetime become

$$\begin{aligned} \rho &= \frac{1}{2r^2 e^\nu} \left[ 2r \mathcal{Q}' (e^\nu - 1) f_{\mathcal{Q}\mathcal{Q}} + f_{\mathcal{Q}} \right. \\ &\quad \times (e^\nu (2 + r\nu' + r\mu') + r\nu' - r\mu' - 2) \\ &\quad \left. - f r^2 e^\nu \right] - \frac{1}{3} f_T (3\rho + P_r + 2P_t) - \frac{q^2}{8\pi r^4}, \end{aligned} \quad (10)$$

$$P_r = \frac{-1}{2r^2 e^v} \left[ 2r Q' f_{QQ}(e^v - 1) + f_Q(e^v(2 + r\mu' + rv') - 2 - rv' - 3r\mu') - fr^2 e^v \right] + \frac{2}{3} f_T(P_t - P_r) + \frac{q^2}{8\pi r^4}, \tag{11}$$

$$P_t = \frac{-1}{4r e^v} \left[ -2r Q' \mu' f_{QQ} + f_Q(2\mu'(e^v - 2) - r\mu'^2 + v'(2e^v + r\mu') - 2r\mu'') - 2fr e^v \right] + \frac{1}{3} f_T(P_r - P_t) - \frac{q^2}{8\pi r^4}. \tag{12}$$

The field equations are complicated because of multivariate functions and their derivatives. We take a particular model as [92]

$$f(Q, T) = \xi Q + \eta T, \tag{13}$$

where  $\xi$  and  $\eta$  are arbitrary constants.

This model enhances our ability to explain gravitational interactions and their connection with matter and energy in greater detail. This model is motivated by its promise to overcome current theoretical limitations and provide a more explanation of the fundamental principles underlying the universe. By adopting this framework, physicists embark on a journey toward unraveling the mysteries of the universe and uncovering the secrets of nature at its most fundamental level. This model stands as a pivotal pursuit in theoretical physics, aiming to unravel the fundamental essence of physical phenomena from the smallest to the largest scales. This model of the  $f(Q, T)$  theory emerges as a crucial endeavor in the realm of theoretical physics, particularly in the pursuit of understanding the fundamental nature of physical phenomena at both macroscopic and microscopic scales. The motivation behind this model of  $f(Q, T)$  theory stems from its potential to overcome existing theoretical limitations, reconcile theoretical predictions with experimental observations and provide a more comprehensive understanding of the fundamental laws governing the universe. By embracing this framework, physicists embark on a journey towards unraveling the mysteries of the cosmos and unlocking the secrets of nature at its most fundamental level. The considered cosmological model has been widely used in the literature [93–98].

The corresponding modified field equations are

$$\rho = \frac{e^{-v}}{24\pi r^4(2\eta - 1)(\eta + 1)} \left[ e^v(3(q^2(1 - 2\eta) + 8\pi r^2\xi(\eta - 1)) - (8\pi r^2\xi + q^2)\eta) + 2\pi r^2\xi(12(\eta - 1)(rv' - 1) + 3r\eta(\mu'(4 - rv' + r\mu') + 2r\mu'')) + \eta(4 + 2r(-v'(2 + r\mu') + \mu'(4 + r\mu') + 2r\mu'')) \right], \tag{14}$$

$$P_r = \frac{e^{-v}}{24\pi r^4(2\eta - 1)(\eta + 1)} \left[ e^v(-3(q^2(1 - 2\eta) + 8\pi r^2\xi(\eta - 1)) + (8\pi r^2\xi + q^2)\eta) + 2\pi r^2\xi(12(\eta - 1 + r\eta v') + 3r(\mu'(4\eta - 4 + r\eta v' - r\eta\mu') - 2r \times \eta\mu'')) + 2\eta(rv'(2 + r\mu') - r(\mu'(4 + r\mu') + 2r\mu'') - 2) \right], \tag{15}$$

$$P_t = \frac{e^{-v}}{24\pi r^4(2\eta - 1)(\eta + 1)} \left[ e^v(3(q^2(1 - 2\eta) + 8\pi r^2\xi\eta) + (q^2 + 8\pi r^2\xi)\eta) + 2\pi r^2\xi(2\eta(rv'(2 + r\mu') - r(\mu'(4 + r\mu') + 2r\mu'') - 2) + 3(r(-v' - \mu') \times (r(\eta - 1)\mu' - 2) + 2r(\eta - 1)\mu'') - 4\eta)) \right]. \tag{16}$$

Here, the metric functions  $(\mu, v)$  must be finite and non-singular to obtain the singular free spacetime. In this regard, we consider Karmarkar condition which is considered as a significant tool to find the exact viable solutions for interior spacetime. This condition is one of many mathematical tools that has been used to comprehend the geometry of cosmic objects, defined as [99]

$$\mathcal{R}_{0303}\mathcal{R}_{1212} = \mathcal{R}_{0101}\mathcal{R}_{2323} + \mathcal{R}_{0113}\mathcal{R}_{0223}, \tag{17}$$

where

$$\begin{aligned} \mathcal{R}_{0101} &= \frac{1}{4}e^\mu(\mu'v' + \mu'^2 + 2\mu''), \\ \mathcal{R}_{2323} &= r^2 \sin^2 \theta(e^{-v} - 1), \\ \mathcal{R}_{0303} &= r \sin^2 \theta \mu' e^{\mu-v}, \quad \mathcal{R}_{1313} = \frac{1}{2}v'r, \\ \mathcal{R}_{0113} &= 0 = \sin^2 \theta \mathcal{R}_{0223}. \end{aligned}$$

Using these values in Eq. (17), we have

$$(v' - \mu')\mu' e^v + 2(1 - e^v)\mu'' + \mu'^2 = 0. \tag{18}$$

Here, we consider a new solution of the metric coefficient as [100]

$$\mu(r) = 2xr^2 + \ln z, \tag{19}$$

where  $x$  and  $z$  are non-negative constants. Using Eqs. (18) and (19), we have

$$v(r) = \ln(1 + y\mu^2 e^\mu), \tag{20}$$

where  $y$  is an integration constant. The unknown parameters in the metric coefficients can be determined by Darmois junction conditions. In the realm of gravitational physics, a single solution to the field equations is not sufficient to completely depict the geometry of cosmic objects. For instance, when dealing with a star, the interior area displays static spherically

symmetric spacetime, whereas the exterior geometry depend upon the matter configuration. The external geometry can be Schwarzschild, Reissner–Nordstrom or Vayia, representing perfect, charged perfect and heat dissipative matter configurations, respectively. The specific constraints called matching conditions must be applied on interior and exterior solutions to obtain a unified depiction of the entire spacetime. Their purpose is to establish a smooth connection between both regions, resulting in one coherent solution at the boundary of the NSs.

We consider the exterior geometry of the NSs as

$$ds_+^2 = \Psi dt^2 - \Psi^{-1} dr^2 - r^2(d\theta^2 + \sin^2\theta d\phi^2), \quad (21)$$

where

$$\Psi = 1 - \frac{2M}{r} + \frac{Q^2}{r^2}.$$

One of the basic matching requirements is the continuity criterion, which asserts that a metric function is assumed to be continuously differentiable at a given point. Applying this criterion enables the derivation of a consistent solution at the boundary ( $r = R$ ) of the NSs. This solution is obtained by establishing equivalence between the interior and exterior metric functions, including their respective derivatives, given as

$$\begin{aligned} g_{tt+} &= g_{tt-} \Rightarrow ze^{2xR^2} = \Psi, \\ g_{rr+} &= g_{rr-} \Rightarrow 1 + 16x^2yR^2ze^{2xR^2} = \Psi^{-1}, \\ g_{tt,r+} &= g_{tt,r-} \Rightarrow 4Rxze^{2R^2x} = \frac{2(MR - Q^2)}{R^3}. \end{aligned} \quad (22)$$

By solving above equations, we get

$$\begin{aligned} x &= -\frac{MR - Q^2}{2R^2(2MR - Q^2 - R^2)}, \\ y &= \frac{R^4(2MR - Q^2)}{4(M^2R^2 - 2MQ^2R + Q^4)}, \\ z &= -\frac{2MR - Q^2 - R^2}{R^2e^{-\frac{MR-Q^2}{2MR-Q^2-R^2}}}. \end{aligned} \quad (23)$$

These parameters play a vital role in the interior of NSs. The mass and radius of the stars under consideration are detailed in Table 1, while the corresponding constants are given in Table 2. Analyzing metric elements is crucial when investigating stellar objects to ensure smoothness and absence of singularities in spacetime. We assume the expression for charge as  $q(r) = Q(\frac{r}{R})^3$  [101] with  $Q = 3$  to examine the effect of charge on the geometry of NSs. Figure 1 demonstrates that both metric components exhibit consistent patterns and indicate an increasing trend which indicates the absence of irregular fluctuations in the spacetime. Thus, we can conclude that the spacetime seems to be uniform and free from singularities, which fulfills the necessary criteria for our investigation.

**Table 1** Values of input parameters

Compact Stellar Objects	$R(km)$	$M_\odot$
Her X-1 [102]	$0.85 \pm 0.15$	$8.1 \pm 0.41$
EXO 1785-248 [103]	$1.30 \pm 0.2$	$10.10 \pm 0.44$
SAX J1808.4-3658 [104]	$0.9 \pm 0.3$	$7.951 \pm 1.0$
4U 1820-30 [105]	$1.58 \pm 0.06$	$9.1 \pm 0.4$
4U 1538-52 [106]	$0.87 \pm 0.07$	$7.866 \pm 0.21$
Vela X-1 [106]	$1.77 \pm 0.08$	$9.56 \pm 0.08$
LMC X-4 [106]	$1.04 \pm 0.09$	$8.301 \pm 0.2$
Cen X-3 [106]	$1.49 \pm 0.08$	$9.178 \pm 0.13$
SMC X-4 [106]	$1.29 \pm 0.05$	$8.831 \pm 0.09$
4U 1608-52 [107]	$1.74 \pm 0.01$	$9.3 \pm 0.10$
PSR J1614-2230 [108]	$1.97 \pm 0.04$	$9.69 \pm 0.2$
PSR J1903+327 [109]	$1.667 \pm 0.021$	$9.48 \pm 0.03$

**Table 2** Values of output parameters

Compact Stellar Objects	$x$	$y$	$z$
Her X-1 (orange line)	0.000161147	9216.97	0.810495
EXO 1785-248 (black line)	0.000701883	720.947	0.614217
SAX J1808.4-3658 (blue line)	0.000239456	5044.6	0.784553
4U 1820-30 (cyan line)	0.0014896	0.0014896	0.466346
4U 1538-52 (magenta line)	0.000173288	9048.16	0.802016
Vela X-1 (gray line)	0.0017267	335.927	0.403078
LMC X-4 (purple line)	0.000515286	1407.2	0.709083
Cen X-3 (yellow line)	0.00125142	446.233	0.508829
SMC X-4 (red line)	0.000935454	615.673	0.591806
4U 1608-52 (pink line)	0.00179681	328.132	0.404899
PSR J1614-2230 (brown line)	0.0021859	284.507	0.329349
PSR J1903+327 (green line)	0.00152105	0.00152105	0.442595

### 3 Viable characteristics of charged neutron stars

In this section, we examine the viable features of NSs using graphical analysis. The following conditions need to be fulfill for viable and stable NSs.

- The metric coefficients need to be monotonically increasing and non-singular at the center of NSs, which ensures that spacetimes does not contain any kind of irregularities.
- The fluid parameters should be maximum at the center and decrease towards the surface boundary. Also,  $P_r(r = R) = 0$  assures that it has a stable denser core.
- The matter gradient must be vanish at the center and then demonstrate negative behavior towards the surface boundary.
- Positive energy bounds ensure the presence of normal matter in the stellar objects

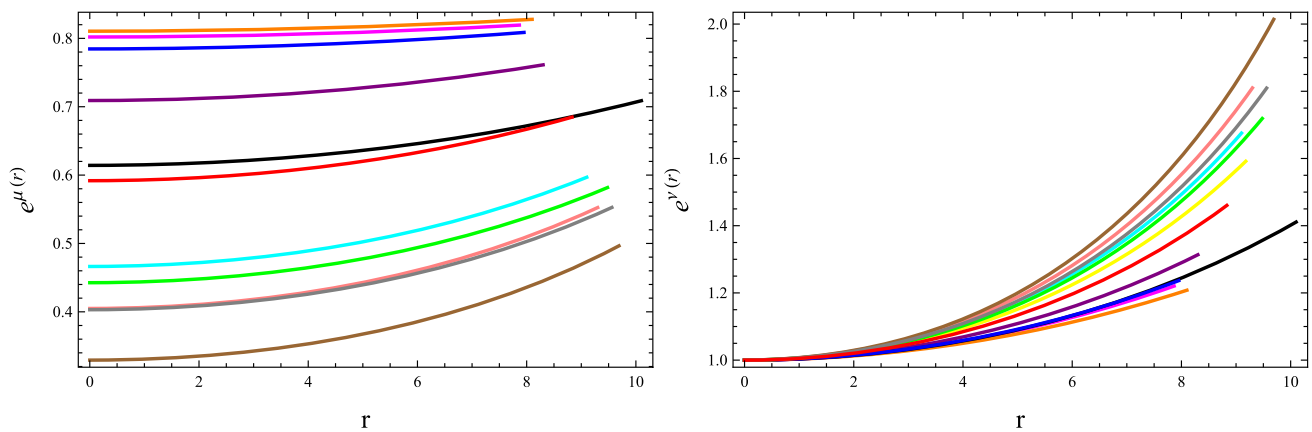


**Fig. 1** Behavior of metric coefficients for different charged NSs

- The EoS parameters must fall in the range of [0,1] for charged NSs to be viable.
- The mass function for NSs needs to be continuous at the core and then show positively increasing behavior.
- The compactness and redshift functions must be less than 0.4 and 5.21, respectively, for viable charged NSs.
- The forces in the NSs must satisfy equilibrium condition to maintain stability.
- For NSs to be stable, the velocities of sound speed should remain in the range of [0,1].

These constraints together provide a framework to understand the behavior of NSs and ensure that their properties are consistent.

### 3.1 Evolution of fluid parameters

The investigation of fluid parameters such as density and pressure is essential to understand the internal features of celestial objects. These matter variables are anticipated to be maximum at the core due to their intense density, counteracting gravitational forces and maintaining the stability of NSs against collapse. Any deviations or negative values could disturb this balance, resulting in structural instability. Comprehending the evolution of fluid parameters and their variation in different theoretical frameworks is crucial not only for astrophysics but also for guiding observational methods and interpreting data from telescopes and other instruments that observe stellar phenomena and structures.

Using Eqs. (14)–(16), we have

$$\rho = \left[ 27r^2 - 63r^2\eta + 240x\pi R^6\xi\eta + 160x^2\pi r^2 R^6\xi\eta - 256x^4y^2z^2e^{4xr^2}r^2(8\pi\xi \times R^6(3 - 2\eta) + 9r^4(7\eta - 3)) + 32x^2yze^{2xr^2}(9r^4(3 - 7\eta) + 12\pi\xi(2\eta - 3)) \right]$$

$$\times R^6 + 16x\pi r^2 R^6\xi(7\eta - 3)) \left] \times \left[ 24\pi(1 + 16x^2yze^{2xr^2}r^2)^2 R^6(1 + \eta) \times (2\eta - 1) \right]^{-1}, \tag{24}$$

$$P_r = \left[ 288x^2yze^{2xr^2}r^4(7\eta - 3) + 2304x^4y^2z^2e^{4xr^2}r^6(7\eta - 3) + 48x\pi R^6\xi \times (8xyz e^{2xr^2}(1 + 2\eta) - 2 - \eta) + r^2(9(7\eta - 3) + 32x^2\pi R^6\xi(16xyz e^{2xr^2} \times (5\eta - 3 - 4xyz e^{2xr^2}(2\eta - 3)) - 5\eta)) \right] \times \left[ 24\pi(1 + 16x^2yze^{2xr^2}r^2)^2 R^6 \times (1 + \eta)(2\eta - 1) \right]^{-1}, \tag{25}$$

$$P_t = \left[ -288x^2yze^{2xr^2}r^4(5\eta - 3) - 2304x^4y^2z^2e^{4xr^2}r^6(5\eta - 3) + 48x\pi R^6\xi \times (8xyz e^{2xr^2}(1 + 2\eta) - 2 - \eta) + r^2(27 - 45\eta + 32x^2\pi R^6\xi((1 + 16xyz \times e^{2xr^2}(16xyz e^{2xr^2} - 1))\eta - 3)) \right] \times \left[ 24\pi(1 + 16x^2yze^{2xr^2}r^2)^2(1 + \eta) \times R^6(2\eta - 1) \right]^{-1}. \tag{26}$$

The plots in Fig. 2 determine that the matter contents are maximum at the core before decreasing, highlighting the dense nature of the NSs. Additionally, the radial pressure in the con-

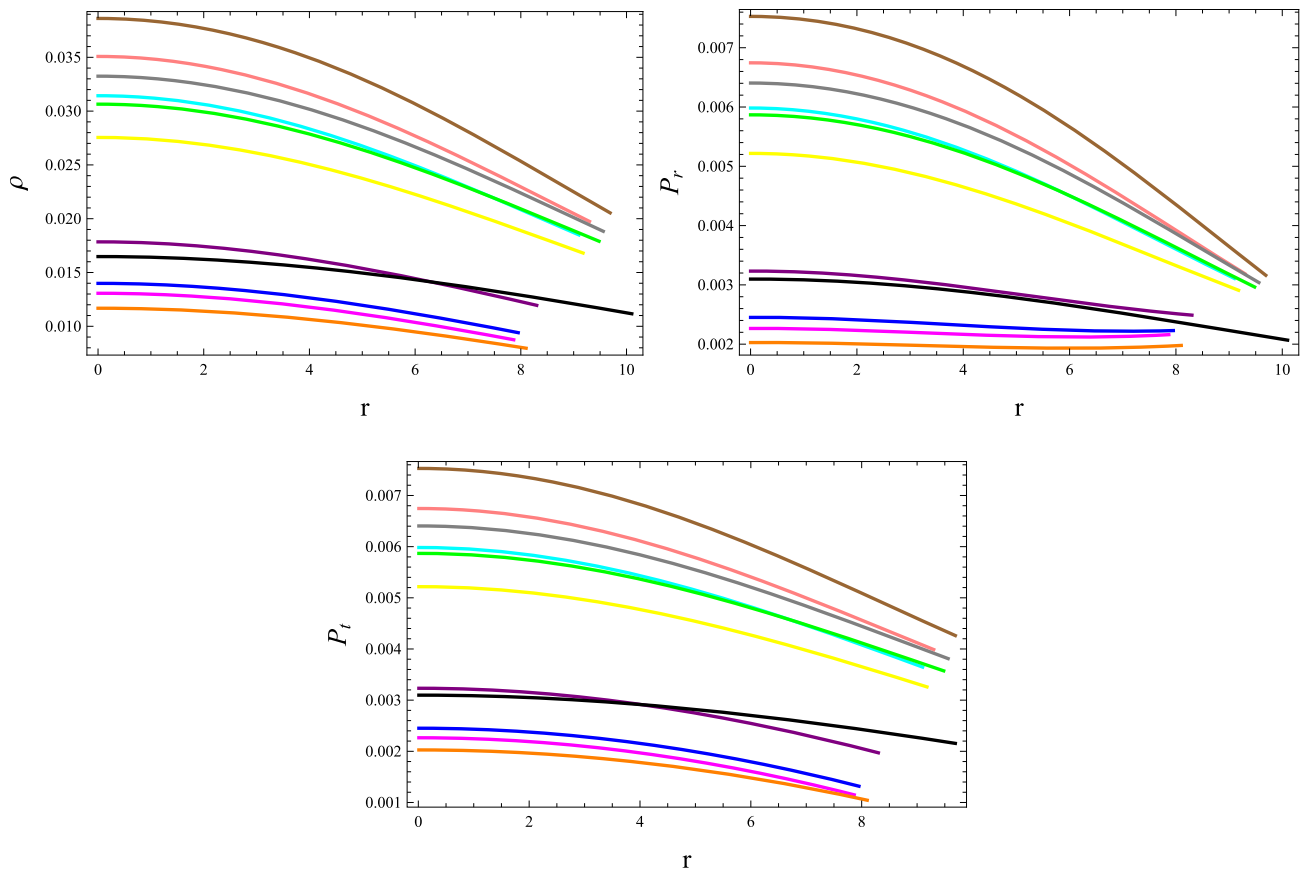


**Fig. 2** Evolution of fluid parameters for different charged NSs

sidered NSs shows a consistent decrease as distance from the center increases until it dissipates at the boundary. Figure 3 manifests that the NSs have highly condensed structures in this framework as they vanish at the core but they become negative thereafter

### 3.2 Anisotropic pressure

An anisotropic fluid refers to a fluid that exhibits different physical properties or behavior in different directions. The term “anisotropic” comes from the Greek words “aniso” meaning unequal or different and “tropos” meaning direction. Anisotropy refers to a difference in pressure along different directions within the NSs. Using Eqs. (25) and (26), we obtain

$$\Delta = P_t - P_r = \left[ r^2(16x^2(\pi R^6\xi + 2yz e^{2xr^2}) \times (-9r^2 - 8x\pi R^6\xi - 8x^2 yze^{2xr^2}) \times (9r^4 - 4\pi R^6\xi)) - 9 \right] \times \left[ 4\pi(1 + 16x^2 yze^{2xr^2} r^2)^2 R^6(1 + \eta) \right]^{-1}.$$

The pressure in a star is isotropic when there are no additional forces or anisotropic effects present. However, in certain situations such as the presence of strong magnetic fields or deviations from isotropy due to gravity or other factors, the pressure becomes anisotropic. One example of anisotropy is the gravitational field around a rotating object. The gravitational field surrounded by rotating massive objects such as a spinning black hole is not uniform in all directions. The gravitational attraction is stronger in some directions than in others, resulting in anisotropic effects. This phenomenon is known as frame-dragging, where the rotation of the object drags the surrounding spacetime along with it. Figure 4 indicates the existence of a repulsive force as the behavior of anisotropy is positive, which plays a crucial role in sustaining large-scale structures and preventing gravitational collapse.

### 3.3 Energy conditions

Astrophysical entities are composed of a variety of materials in their composition and it is important to differentiate the types of substances (exotic/ordinary) present in celestial objects. Energy constraints are necessary to examine the viable fluid configurations in the system. These limitations

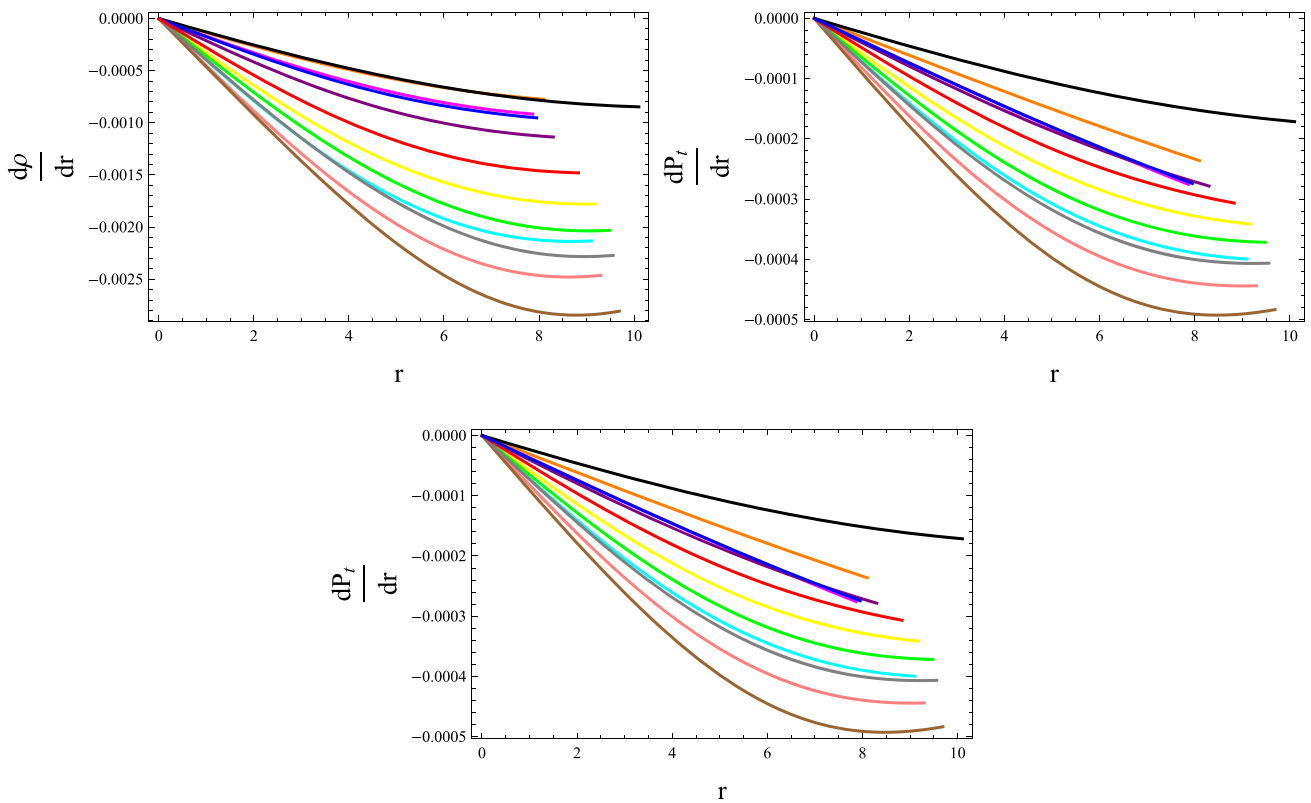


**Fig. 3** Evolution of gradient of fluid parameters versus radial coordinate

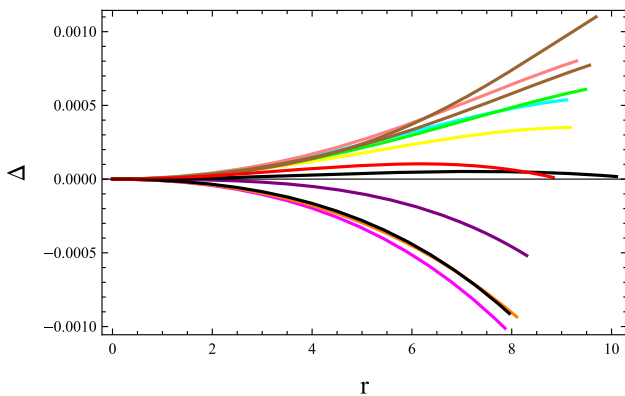


**Fig. 4** Behavior of anisotropy versus radial coordinate

play a crucial role in investigating the presence of specific cosmic formations and understanding how matter and energy interact under the influence of gravity. These constraints manifest the physical viability of the matter configuration in the cosmic objects. The ECs are characterized into four types as

• **Null Energy Condition**

This condition states that for any null vector, the energy density measured along that vector is non-negative.

Mathematically, this condition can be expressed as

$$0 \leq P_r + \rho, \quad 0 \leq P_t + \rho + \frac{q^2}{4\pi r^4}.$$

This condition does not provide any direct information about the relationship between the energy density and pressure. It allows for cases where the pressure may be larger or smaller than the energy density.

• **Strong Energy Condition**

This constraint demonstrates that the sum of three times the energy density and the pressure in any given direction is non-negative. Mathematically, it can be expressed as

$$0 \leq \rho + P_r, \quad 0 \leq \rho + P_t + \frac{q^2}{4\pi r^4},$$

$$0 \leq \rho + P_r + 2P_t + \frac{q^2}{4\pi r^4}.$$

• **Dominant Energy Condition**

The dominant energy condition manifests that for any vector field, the energy density must be non-negative and the vector must be time-like or null-like. Mathematically,

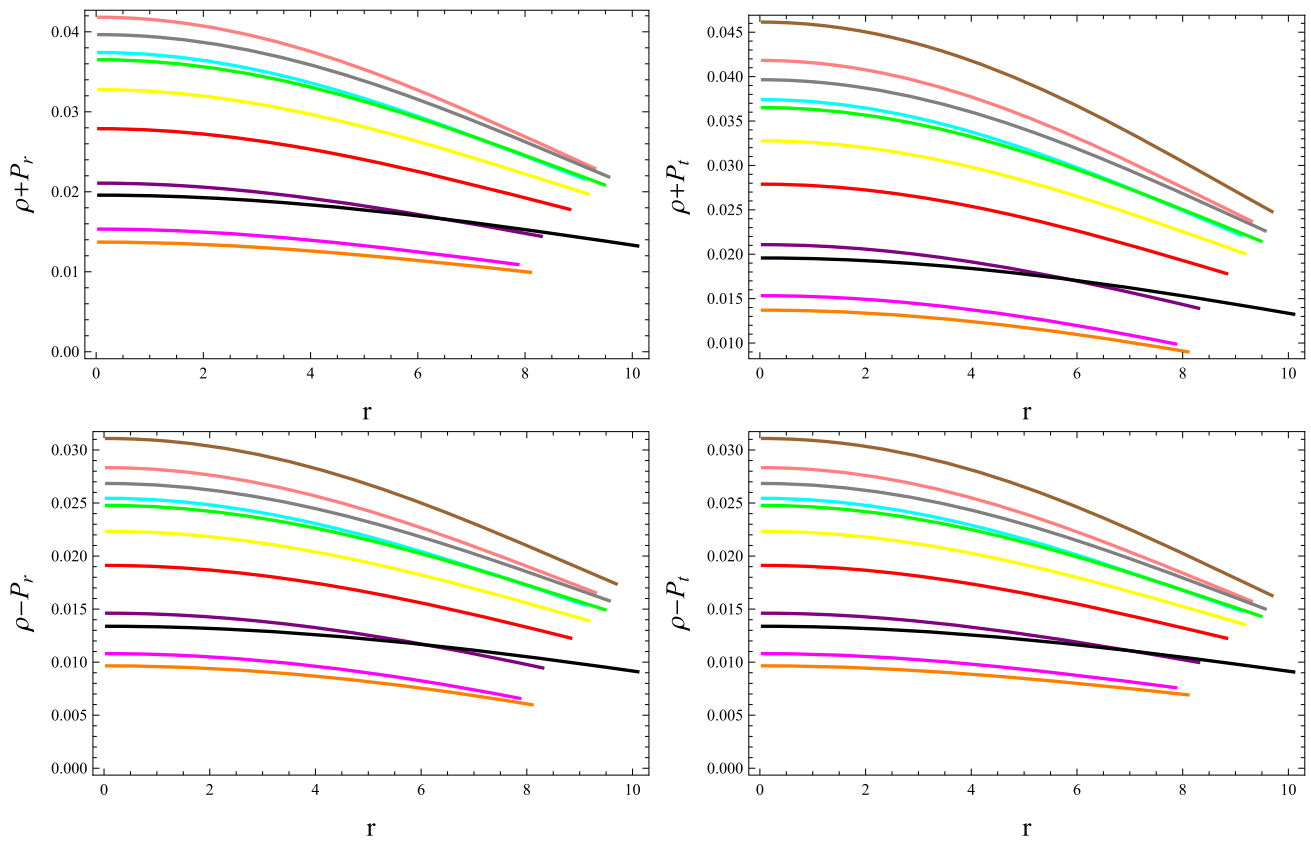


Fig. 5 Graphs of energy conditions for different charged NSs

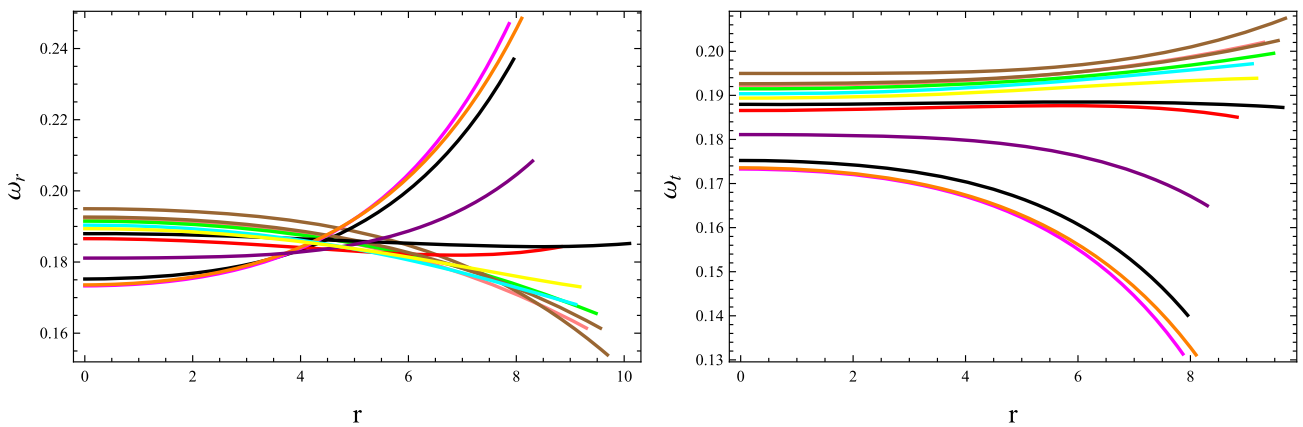


Fig. 6 Graph of EoS parameters for different charged NSs

it can be written as

$$0 \leq \rho - P_r, \quad 0 \leq \rho - P_t + \frac{q^2}{4\pi r^4}.$$

• **Weak Energy Condition**

This condition determines that the energy density measured by any observer must be non-negative. Mathematically, for all vector fields, this condition can be written

as

$$0 \leq \rho + \frac{q^2}{4\pi r^4}, \quad 0 \leq \rho + P_r, \quad 0 \leq \rho + P_t + \frac{q^2}{4\pi r^4}.$$

The weak energy condition is more restrictive than the null energy condition as it requires the energy density to be non-negative for all observers.

Scientists can gain insights into the nature and behavior of cosmic structures by analyzing these energy bounds and their effects on the stress-energy tensor, contributing to our understanding of the dynamics and evolution of the universe. Figure 5 shows that the considered NSs are viable as all energy constraints are satisfied in the presence of modified terms.

### 3.4 Analysis of state parameters

The EoS parameters explain how energy density is related to anisotropic pressure in different types of systems. The radial component ( $\omega_r = \frac{P_r}{\rho}$ ) and transverse component ( $\omega_t = \frac{P_t}{\rho}$ ) of EoS parameters must satisfy range [0,1] for viable stellar objects. Using Eqs. (24)–(26), we have

$$\omega_r = \left[ \begin{aligned} & -288x^2yz e^{2xr^2} r^4(7\eta - 3) \\ & -2304x^4y^2z^2 e^{4xr^2} r^6(7\eta - 3) + 48x\pi\xi R^6 \\ & \times (2 + \eta - 8xyz e^{2xr^2} (1 + 2\eta)) \\ & + r^2(27 - 63\eta + 32x^2\pi R^6\xi(16xyz e^{2xr^2} \\ & \times (3 - 5\eta + 4xyz e^{2xr^2} (2\eta - 3))5\eta)) \end{aligned} \right] \times \left[ \begin{aligned} & 63r^2\eta - 27r^2 - 240x\pi R^6\xi\eta 160x^2 \\ & -\pi r^2 R^6\xi\eta + 256x^4y^2z^2 e^{4xr^2} r^2 \\ & \times (8\pi R^6\xi(3 - 2\eta) + 9r^4(7\eta - 3)) + 32x^2 \\ & \times yz e^{2xr^2} (16x\pi r^2 R^6\xi(3 - 7\eta) \\ & + 12\pi R^6\xi(3 - 2\eta) + 9r^4(7\eta - 3)) \end{aligned} \right]^{-1}, \tag{27}$$

$$\omega_t = \left[ \begin{aligned} & 288x^2yz e^{2xr^2} r^4(7\eta - 3) \\ & + 2304x^4y^2z^2 e^{4xr^2} r^6(7\eta - 3) + 48x\pi R^6\xi(2 \\ & + \eta - 8xyz e^{2xr^2} (1 + 2\eta)) + r^2(9(5\eta - 3) \\ & - 32x^2\pi R^6\xi(5\eta + 16xyz e^{2xr^2} \\ & \times (3 - 5\eta + 4xyz e^{2xr^2} (2\eta - 3)))) \end{aligned} \right] \times \left[ \begin{aligned} & 63r^2\eta - 27r^2 - 240x\pi R^6\xi\eta - 160x^2 \\ & \times \pi r^2 R^6\xi\eta + 256x^4y^2z^2 e^{4xr^2} r^2 \\ & \times (8\pi R^6\xi(3 - 2\eta) + 9r^4(7\eta - 3)) + 32x^2yz \\ & \times e^{2xr^2} (16x\pi r^2 R^6\xi(3 - 7\eta) \\ & + 12\pi R^6\xi(3 - 2\eta) + 9r^4(7\eta - 3)) \end{aligned} \right]^{-1}, \tag{28}$$

Figure 6 determines that the EoS parameters satisfied the required limit for the NSs under considerations.

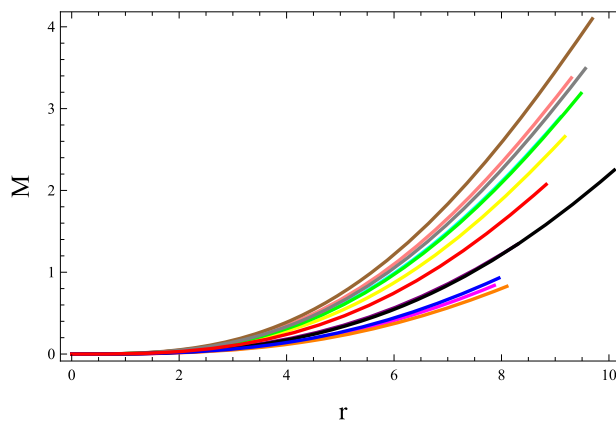


Fig. 7 Graph of mass function for different charged NSs

### 3.5 Evolution of different physical aspects

The mass of stellar objects is defined as [110]

$$M = 4\pi \int_0^R r^2 \rho dr. \tag{29}$$

Figure 7 demonstrates that the mass function is monotonically increasing and  $M \rightarrow 0$  as  $r \rightarrow 0$ , suggesting that there are no abnormalities or irregularities in the mass distribution. Various physical characteristics can be assessed to analyze the structural configuration of cosmic objects. A fundamental factor in assessing the viability of NSs is the compactness function, represented by ( $u = \frac{M}{R}$ ). This function offers insights into the distribution of mass relative to the radius of a NS and its concentration. The compactness factor is a physical parameter that provides a quantitative measure of how densely packed the mass is within a given radius. This factor is calculated by dividing the mass of the structure by its radius. There is a specific limit for the mass to radius ratio that was proposed by Buchdhal for a physically relevant model [111]. According to his criterion, the mass-radius ratio should be less than  $\frac{4}{9}$  for viable charged NSs.

The surface redshift is a significant factor in the study of NSs as it provides important information about the brightness and energy of light emitted from their surfaces, which is caused by the gravitational redshift experienced at a star’s surface due to its strong gravity. It is a phenomenon which explains the change in frequency (and hence the wavelength) of light or other electromagnetic radiations as it travels away from a gravitational field. It occurs when the source of light or radiations is in a stronger gravitational field compared to the observer. As the light moves away from the gravitational field, it loses energy and thus its wavelength is increased, causing it to shift towards the red end of the electromagnetic spectrum. It is denoted by  $Z_s$  and mathematically expressed

as

$$Z_s = -1 + \frac{1}{\sqrt{1-2u}}. \quad (30)$$

In case of anisotropic configuration, the redshift at the surface must satisfy the specific condition as  $Z_s < 5.211$  for NSs to be viable [112]. The graph in Fig. 8 demonstrates that both compactness and redshift functions meet the essential feasibility criteria.

#### 4 Equilibrium and stability analysis

It is important to comprehend the behavior and physical characteristics of celestial objects in the field of gravitational physics. Equilibrium and stability play a significant role in this endeavor. Equilibrium represents a balance state where the resultant of all forces acting on a system vanishes. The stability of cosmic formations is significant to develop their reliability and coherence. Scientists have investigated the conditions that determine the stability of these formations against various forms of oscillations. To assess the stability of NSs, researchers use the methods such as causality constraint and Herrera cracking approach, providing important perspectives on the structural integrity of astronomical objects.

##### 4.1 Analysis of different forces

Here, we consider the TOV equation, which offers a mathematical representation of how pressure counteracts gravitational collapse to maintain equilibrium [113]. The TOV equation is derived by considering a static spherically symmetric object and solving the Einstein field equations. This equation provides us with valuable information regarding the forces that act upon a system and keeps it stable. It is crucial to study the internal structure and properties of dense stars.

The corresponding equation is defined as

$$\frac{M_G(r)e^{\frac{\mu-\nu}{2}}}{r^2}(\rho + P_r) + \frac{dP_r}{dr} - \frac{2}{r}(P_t - P_r) = 0, \quad (31)$$

where

$$M_G(r) = 4\pi \int e^{\frac{\mu+\nu}{2}} (\mathcal{T}_0^0 - \mathcal{T}_1^1 - \mathcal{T}_2^2 - \mathcal{T}_3^3) r^2 dr.$$

Its solution yields

$$M_G(r) = \frac{1}{2} r^2 e^{\frac{\nu-\mu}{2}} \mu'.$$

Inserting this value in Eq. (31), we have

$$\frac{1}{2} \mu'(\rho + P_r) + P_r' - \frac{2\Delta}{r} = 0.$$

This equation presents a model to understand the internal structure of stars, encompassing their density distribution and pressure profile. It demonstrates the influence of distinct forces on the system, i.e., gravitational ( $F_g = \frac{\mu'(\rho+P_r)}{2}$ ), hydrostatic ( $F_h = \frac{dP_r}{dr}$ ) and anisotropic ( $F_a = \frac{2(P_t-P_r)}{r}$ ) forces acting on the system. Using Eqs. (24)–(26), we obtain

$$F_g = \left[ 8x^2 r (1 + 8xyz e^{2xr^2} (1 + 4xr^2)) \xi \right] \times \left[ (1 + 16x^2 yz e^{2xr^2} r^2)^2 (1 + \eta) \right]^{-1}, \quad (32)$$

$$F_h = \left[ r(9(7\eta - 3) + 16x^2(256x^4 y^3 z^3 e^{6xr^2} r^2 \times (8\pi R^6 \xi(2\eta - 3) + 9r^4(7\eta - 3)) - 16x^2 y^2 z^2 e^{4xr^2} (8\pi R^6 \xi(3 + 14\eta) + 16x\pi r^2 R^6 \xi(20\eta - 9) + r^4(81 - 189\eta + 64x^2 \pi R^6 \xi(5\eta - 3))) + yz e^{2xr^2} \times (640x^3 \pi r^4 R^6 \xi \eta + 16x\pi R^6 \xi(9 + 22\eta) + 3r^2(9(7\eta - 3) + 32x^2 \pi R^6 \xi(2 + 7\eta))) \right]$$

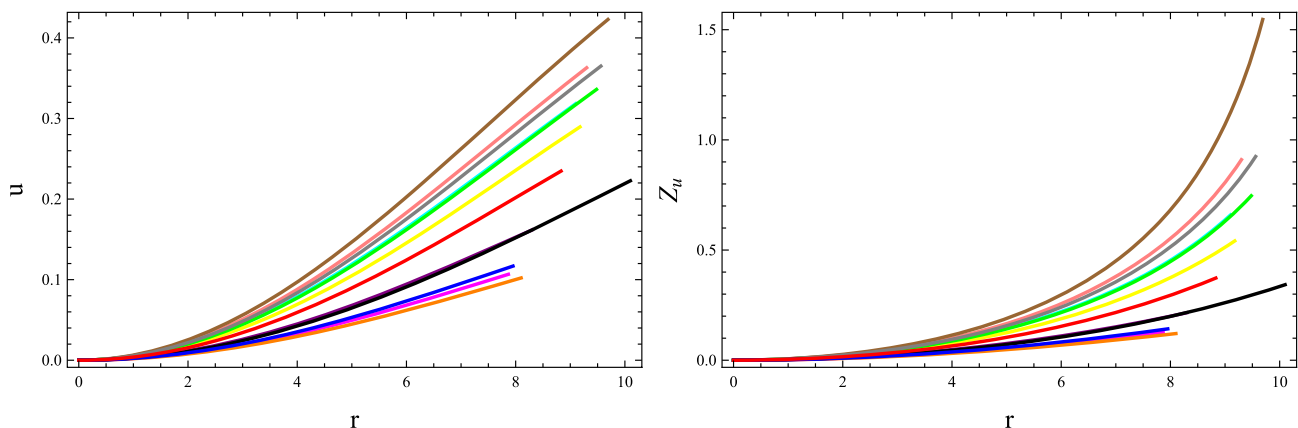


**Fig. 8** Behavior of compactness and redshift for different charged NSs

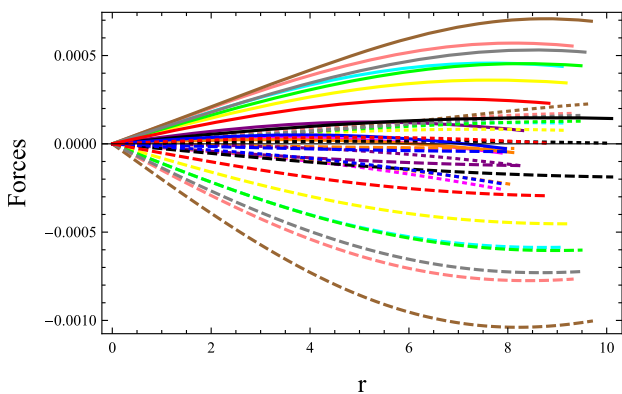


**Fig. 9** Plot of gravitational force (dashed line), hydrostatic force (solid line) and anisotropic force (dotted line)

$$-10\pi R^6 \xi \eta) \Big] \Big[ 12\pi(1 + 16x^2 yz \times e^{2xr^2} r^2)^3 R^6(1 + \eta)(2\eta - 1) \Big]^{-1}, \tag{33}$$

$$F_a = \Big[ r(9 + 16x^2(2yz e^{2xr^2}(9r^2 + 8x\pi R^6 \xi + 8x^2 yz e^{2xr^2}(9r^4 - 4\pi R^6 \xi)) - \pi R^6 \xi)) \Big] \Big[ 2\pi(1 + 16x^2 yz e^{2xr^2} r^2)^2 R^6(1 + \eta) \Big]^{-1}. \tag{34}$$

Figure 9 shows that the charged stellar objects are in equilibrium phase as sum of  $F_g$ ,  $F_h$  and  $F_a$  is zero.

### 4.2 Causality constraint

The stability of NSs can be evaluated by considering the causality constraint, which states that nothing can travel faster than the speed of light. In order to maintain stable configurations, both the radial and tangential velocities of sound ( $u_r = \frac{dP_r}{d\rho}$  and  $u_t = \frac{dP_t}{d\rho}$ ) must fall in the range of 0 to 1 [114]. These characteristics related to sound speed play a critical role in ensuring the stability of NSs.

$$u_r = \Big[ 27 - 63\eta + 16x^2(10\pi R^6 \xi \eta - 256x^4 y^3 z^3 e^{6xr^2} r^2(8\pi R^6 \xi(2\eta - 3) + 9r^4 \times (7\eta - 3)) + 16x^2 y^2 z^2 e^{4xr^2}(8\pi R^6 \xi(3 + 14\eta) + 16x\pi r^2 R^6 \xi(20\eta - 9) + r^4 \times (81 - 189\eta + 64x^2 \pi R^6 \xi(5\eta - 3))) - yz e^{2xr^2}(640x^3 \pi r^4 R^6 \xi \eta + 16x\pi \xi \times R^6(9 + 22\eta) + 3r^2(9(7\eta - 3) + 32x^2 \pi R^6 \xi(2 + 7\eta)))) \Big] \Big[ 9(7\eta - 3) + 16x^2(256x^4 y^3 z^3 e^{6xr^2} r^2(8\pi R^6 \xi(2\eta - 3) + 9r^4(7\eta - 3)) + 16x^2 y^2 z^2 e^{4xr^2} \times (40\pi R^6 \xi(2\eta - 3) + r^4(27 + 64x^2 \pi R^6 \xi) \times (7\eta - 3) + 16x\pi r^2 R^6 \xi(16\eta - 9) + yz e^{2xr^2}(640x^3 \pi r^4 R^6 \xi \eta + 80x\pi R^6 \xi(3 + 2\eta) + 3r^2(9(7\eta - 3) + 32x^2 \pi R^6 \xi(2 + 7\eta)))) - 10\pi R^6 \xi \eta) \Big]^{-1}. \tag{36}$$

$$\times e^{4xr^2}(40\pi R^6 \xi(2\eta - 3) + r^4(27 + 64x^2 \pi R^6 \xi)(7\eta - 3) + 16x\pi r^2 R^6 \times \xi(16\eta - 9)) + yz e^{2xr^2} \times (640x^3 \pi r^4 R^6 \xi \eta + 80x\pi R^6 \xi(3 + 2\eta) + 3r^2(9(7\eta - 3) + 32\pi \xi R^6 x^2(2 + 7\eta))) - 10\pi R^6 \xi \eta) \Big]^{-1}, \tag{35}$$

$$u_t = \Big[ 9(5\eta - 3) + 16x^2(256x^4 y^3 z^3 e^{6xr^2} r^2 \times (32\pi R^6 \xi \eta + 9r^4(5\eta - 3)) - 16x^2 \times y^2 z^2 e^{4xr^2}(16x\pi r^2 R^6 \xi(4\eta - 3) - 16\pi R^6 \xi(3 + 4\eta) + r^4(81 - 135\eta + 64 \times \pi x^2 R^6 \xi \eta)) + yz e^{2xr^2} \times (128x^3 \pi r^4 R^6 \xi(\eta - 3) - 80x\pi R^6 \xi(3 + 2\eta) - 3r^2 \times (27 - 45\eta + 32x^2 \pi R^6 \xi(5 + \eta))) - 2\pi R^6 \xi(\eta - 3) \Big] \Big[ 9(7\eta - 3) + 16x^2 \times (256x^4 y^3 z^3 e^{6xr^2} r^2(8\pi R^6 \xi(2\eta - 3) + 9r^4(7\eta - 3)) + 16x^2 y^2 z^2 e^{4xr^2} \times (40\pi R^6 \xi(2\eta - 3) + r^4(27 + 64x^2 \pi R^6 \xi) \times (7\eta - 3) + 16x\pi r^2 R^6 \xi(16\eta - 9) + yz e^{2xr^2}(640x^3 \pi r^4 R^6 \xi \eta + 80x\pi R^6 \xi(3 + 2\eta) + 3r^2(9(7\eta - 3) + 32x^2 \pi R^6 \xi(2 + 7\eta)))) - 10\pi R^6 \xi \eta) \Big]^{-1}. \tag{36}$$

Figure 10 shows that the considered NSs meet the required condition. Thus, this modified theory supports the existence of physically viable and stable NSs.

### 4.3 Herrera cracking approach

The analysis of solution’s stability is based on a mathematical method called the cracking approach ( $0 \leq |u_t - u_r| \leq 1$ ), which was developed by Herrera [115]. Satisfying this condition indicates stable cosmic structures capable of long-term existence, otherwise, it signifies instability and will collapse. This method enables researchers to determine the stability of cosmic structures, which is essential for understanding their behavior in the universe. Figure 11 depicts the fulfillment of the cracking condition as the both radial and tangential sound speed components lie in the range [0,1], which ensures the stability of the stellar objects under consideration.

## 5 Final outcomes

This research investigates the feasibility and stability of NSs in the extended symmetric teleparallel theory. The main aim is to investigate whether incorporating non-metricity into the gravitational field equations results in feasible solutions for NSs. Introducing these terms to the theory presents

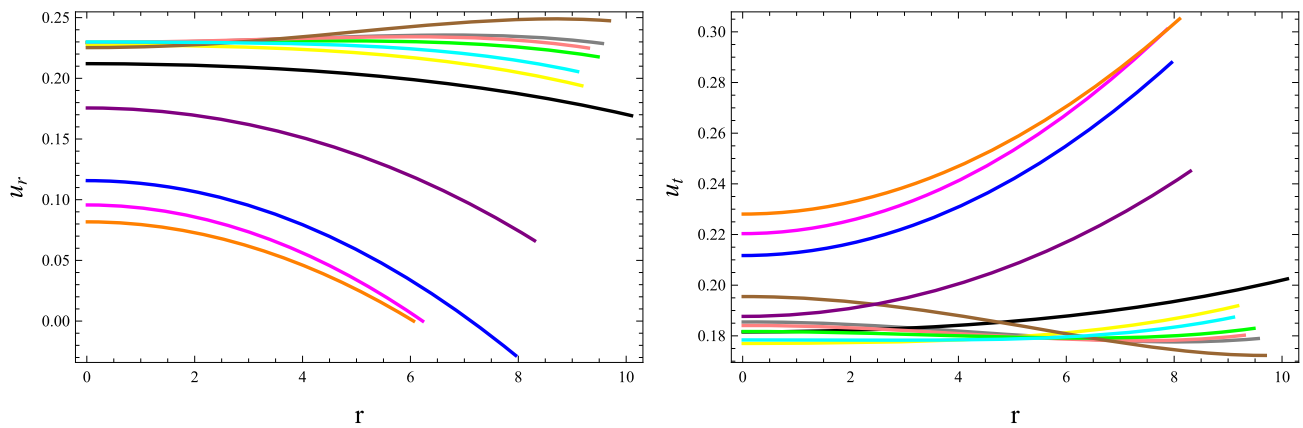


**Fig. 10** Plots of sound speed components for different charged NSs

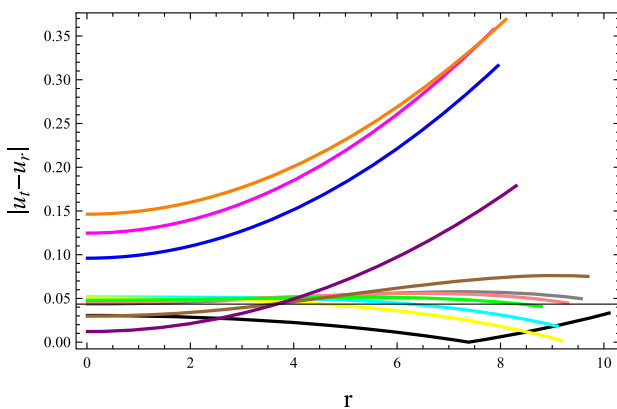


**Fig. 11** Plot of Herrera cracking for different charged NSs

new insights into how matter and geometry interact under extreme gravitational circumstances. Furthermore, we have conducted a graphical analysis of various physical characteristics to verify the viability of the NSs in the proposed theoretical framework. In addition, we have assessed stability through methods that incorporate sound speed.

The metric functions describe the geometry of spacetime. Consistent and non-singular metric coefficients ensure that spacetime is smooth and free from singularities (Fig. 1). This smoothness is fundamental for any viable cosmological model. The matter contents are dense at the center of the considered NSs, indicating a stable core (Fig. 2). This behavior of fluid parameters is important for maintaining the structural integrity of NSs. Moreover, the decrease in fluid variables as we move towards the boundary indicates a viable configuration of the NSs. The absence of radial pressure at the surface boundary confirms the physical viability of these objects. The matter contents exhibit a negative gradient, indicating a dense profile of the suggested stellar objects (Fig. 3).

The anisotropy diminishes at the core of NSs which is a desirable feature for maintaining the stability of the NSs

(Fig. 4). Furthermore, the outward direction of anisotropic pressure is a crucial characteristic for compact stellar formations. All energy constraints are positive (Fig. 5), affirming the presence of ordinary matter in NSs. Figure 6 demonstrates the validity of the model under consideration as the EoS parameter falls in a range from 0 to 1. The mass function shows an increasing trend as the radial coordinate increases, indicating a feasible mass distribution in the NSs (Fig. 7). Additionally, the compactness factor is less than  $4/9$  and redshift is less than 5.2, supporting the viability of these compact structures (Fig. 8). The stability limits guarantee the existence of stable NSs in this framework as illustrated in Figs. 9, 10 and 11.

We have analyzed various physical quantities and stability criteria to check whether NSs could exist in the theoretical framework provided by  $f(Q, T)$  theory. Our investigation into the physical characteristics reveals the dense nature of NSs and confirms the presence of viable and stable NSs in this modified framework. In the context of  $f(R, T^2)$  theory, previous studies have shown that NSs are neither physically feasible nor stable at their centers [116]. However, our findings demonstrate that all considered stars display both physical feasibility and stability at their central positions under  $f(Q, T)$  theory. Therefore, the solutions we have derived yield stable formations of anisotropic NSs.

**Acknowledgments** Baiju Dayanandan acknowledges support from the administration of the University of Nizwa.

**Data Availability Statement** This manuscript has no associated data. [Author's comment: This is a theoretical study and no experimental data.]

**Code Availability Statement** This manuscript has no associated code/software. [Author's comment: This is a theoretical study and no experimental data.]

**Open Access** This article is licensed under a Creative Commons Attribution 4.0 International License, which permits use, sharing, adaptation, distribution and reproduction in any medium or format, as long as you

give appropriate credit to the original author(s) and the source, provide a link to the Creative Commons licence, and indicate if changes were made. The images or other third party material in this article are included in the article's Creative Commons licence, unless indicated otherwise in a credit line to the material. If material is not included in the article's Creative Commons licence and your intended use is not permitted by statutory regulation or exceeds the permitted use, you will need to obtain permission directly from the copyright holder. To view a copy of this licence, visit <http://creativecommons.org/licenses/by/4.0/>.  
Funded by SCOAP<sup>3</sup>.

## References

- H.S. Weyl, *Preuss. Akad. Wiss.* **1**, 465 (1918)
- J.B. Jimenez, I. Heisenberg, L.T. Koivisto, *Phys. Rev.* **98**, 044048 (2018)
- M. Adak et al., *Turk. J. Phys.* **29**, 1 (2005)
- M. Adak, *Turk. J. Phys.* **30**, 379 (2006)
- S.K. Maurya et al., *Fortschr. Phys.* **70**, 2200061 (2022)
- A.D. Felice, S.R. Tsujikawa, *Living Rev. Relativ.* **13**, 3 (2010)
- T. Harko et al., *Phys. Rev. D* **84**, 024020 (2011)
- M. Sharif, M.Z. Gul, *Eur. Phys. J. Plus* **133**, 345 (2018)
- M. Sharif, M.Z. Gul, *Mod. Phys. Lett. A* **36**, 2150214 (2021)
- M. Sharif, M.Z. Gul, *Ann. Phys.* **465**, 169674 (2024)
- M. Sharif, M.Z. Gul, *Phys. Scr.* **99**, 065036 (2024)
- M.Z. Gul, M. Sharif, I. Hashim, *Phys. Dark Universe* **45**, 101537 (2024)
- M.Z. Gul, M. Sharif, *Phys. Scr.* **99**, 055036 (2024)
- M.Z. Gul, M. Sharif, *Chin. J. Phys.* **88**, 388 (2024)
- M.Z. Gul, M. Sharif, *New Astron.* **106**, 102137 (2024)
- Y. Xu et al., *Eur. Phys. J. C* **79**, 708 (2019)
- Y. Xu et al., *Eur. Phys. J. C* **80**, 449 (2020)
- S. Arora, P.K. Sahoo, *Phys. Scr.* **95**, 095003 (2020)
- A.S. Agrawal et al., *Phys. Dark Universe* **33**, 100863 (2021)
- N. Godani, G.C. Samanta, *Int. J. Geom. Methods Mod. Phys.* **18**, 2150134 (2021)
- A. Najera, A. Fajardo, *Phys. Dark Universe* **34**, 100889 (2021)
- S. Arora, J.R.L. Santos, P.K. Sahoo, *Phys. Dark Universe* **31**, 100790 (2021)
- B.K. Shukla et al., *Mod. Phys. Lett. A* **39**, 2450005 (2024)
- W. Baade, F. Zwicky, *Phys. Rev.* **46**, 76 (1934)
- T. Gold, *Nature* **218**, 731 (1968)
- R.L. Bowers, E.P.T. Liang, *Astrophys. J.* **188**, 657 (1974)
- L. Herrera, N.O. Santos, *Phys. Rep.* **286**, 53 (1997)
- K. Dev, M. Gleiser, *Gen. Relativ. Gravit.* **39**, 1793 (2002)
- M.K. Mak, T. Harko, *Int. J. Mod. Phys. D* **13**, 156 (2004)
- M. Kalam et al., *Eur. Phys. J. C* **72**, 2248 (2012)
- F. Rahaman et al., *Gen. Relativ. Gravit.* **44**, 107 (2012)
- Z. Yousaf et al., *Eur. Phys. J. C* **77**, 691 (2017)
- P. Bhar et al., *Int. J. Mod. Phys. D* **26**, 1750078 (2017)
- M. Zubair, A. Ditta, S. Waheed, *Eur. Phys. J. Plus* **136**, 508 (2021)
- Z. Yousaf et al., *Phys. Dark Universe* **36**, 101015 (2022)
- Z. Yousaf, M.Z. Bhatti, S. Khan, *Eur. Phys. J. Plus* **137**, 322 (2022)
- Z. Yousaf, *Universe* **8**, 131 (2022)
- Z. Yousaf et al., *Entropy* **24**, 150 (2022)
- B. Dayanandan et al., *Chin. J. Phys.* **82**, 155 (2023)
- Z. Yousaf et al., *Ann. Phys.* **458**, 169448 (2023)
- S. Khan, Z. Yousaf, *Phys. Scr.* **99**, 055303 (2024)
- G. Mustafa et al., *Chin. J. Phys.* **88**, 938 (2024)
- Z. Yousaf, *Phys. Scr.* **97**, 025301 (2022)
- S. Khan, A. Adeel, Z. Yousaf, *Eur. Phys. J. C* **84**, 572 (2024)
- Z. Yousaf et al., *Chin. J. Phys.* **88**, 406 (2024)
- A. Kunkel, T. Chiueh, B.M. Schafer, *Mon. Not. R. Astron. Soc.* **527**, 10538 (2024)
- Z. Yousaf et al., arXiv preprint [arXiv:2405.08354](https://arxiv.org/abs/2405.08354)
- T. Dome, R. Azhar, A. Fialkov, *Mon. Not. R. Astron. Soc.* **527**, 10397 (2024)
- T. Naz et al., *Chin. J. Phys.* **89**, 871 (2024)
- Z. Yousaf et al., *Chin. J. Phys.* **89**, 1595 (2024)
- Z. Yousaf, K. Bamba, M.Z.U.H. Bhatti, *Phys. Rev. D* **95**, 024024 (2017)
- M.Z. Bhatti, Z. Yousaf, M. Ilyas, *Eur. Phys. J. C* **77**, 9 (2017)
- S.K. Maurya, K.N. Singh, R. Nag, *Chin. J. Phys.* **74**, 313 (2021)
- A.R. Athar, M. Ilyas, B. Masud, *Int. J. Geom. Methods Mod. Phys.* **20**, 2350003 (2023)
- P. Bhar, J.M. Pretel, *Phys. Dark Universe* **42**, 101322 (2023)
- M. Ilyas, A.R. Athar, A. Bibi, *New Astron.* **103**, 102053 (2023)
- A. Majeed, G. Abbas, M.R. Shahzad, *New Astron.* **102**, 102039 (2023)
- A. Malik et al., *Chin. J. Phys.* **89**, 613 (2024)
- A.M. Albalahi et al., *Eur. Phys. J. C* **84**, 9 (2024)
- A. Malik et al., *Eur. Phys. J. Plus* **139**, 101 (2024)
- A. Ditta, X. Tiecheng, *Phys. Scr.* **99**, 025012 (2024)
- M.Z. Bhatti et al., *Int. J. Mod. Phys. D* **27**, 1850044 (2018)
- Z. Yousaf et al., *Eur. Phys. J. C* **78**, 13 (2018)
- S. Dey, A. Chanda, B.C. Paul, *Eur. Phys. J. Plus* **136**, 228 (2021)
- P. Rej, P. Bhar, M. Govender, *Eur. Phys. J. C* **81**, 316 (2021)
- M. Ilyas, *Int. J. Mod. Phys. A* **36**, 2150165 (2021)
- M. Ilyas, A.R. Athar, B. Masud, *Int. J. Geom. Methods Mod. Phys.* **18**, 2150152 (2021)
- R.H. Lin, X.H. Zhai, *Phys. Rev. D* **103**, 124001 (2021)
- M.F. Shamir, A. Malik, *Chin. J. Phys.* **69**, 312 (2021)
- K.P. Das, U. Debnath, A. Ashraf, M. Khurana, *Phys. Dark Universe* **43**, 101398 (2024)
- A. Malik, A. Arif, M.F. Shamir, *Eur. Phys. J. Plus* **139**, 67 (2024)
- G.G. Nashed, S. Capozziello, *Eur. Phys. J. C* **81**, 481 (2021)
- M.F. Shamir, A. Rashid, *Int. J. Geom. Methods Mod. Phys.* **20**, 2350026 (2023)
- M. Ilyas, D. Ahmad, *Chin. J. Phys.* **88**, 901 (2024)
- P. Rej, P. Bhar, *New Astron.* **105**, 102113 (2024)
- G. Mustafa et al., *Eur. Phys. J. C* **80**, 26 (2020)
- G. Mustafa et al., *Phys. Rev. D* **101**, 104013 (2020)
- A. Ditta et al., *Eur. Phys. J. C* **81**, 880 (2021)
- G. Mustafa et al., *Phys. Dark Universe* **31**, 100747 (2021)
- F. Javed et al., *Eur. Phys. J. C* **83**, 513 (2023)
- F. Javed et al., *Nucl. Phys. B* **990**, 116180 (2023)
- F. Javed et al., *Fortschr. Phys.* **2023**, 2200214 (2023)
- F. Javed et al., *Ann. Phys.* **458**, 169464 (2023)
- M. Adeel et al., *Mod. Phys. Lett. A* **38**, 2350152 (2023)
- S. Rani et al., *Int. J. Geom. Methods Mod. Phys.* **21**, 2450033 (2024)
- M.Z. Gul et al., *Eur. Phys. J. C* **84**, 8 (2024)
- M.Z. Gul, M. Sharif, A. Arooj, *Fortschr. Phys.* **72**, 2300221 (2024)
- M.Z. Gul, M. Sharif, A. Arooj, *Phys. Scr.* **99**, 045006 (2024)
- M.Z. Gul, M. Sharif, A. Arooj, *Gen. Relativ. Gravit.* **56**, 45 (2024)
- L. Herrera, N.O. Santos, *Phys. Rep.* **286**, 53 (1997)
- P.H.R.S. Moraes, P.K. Sahoo, *Phys. Rev. D* **97**, 024007 (2018)
- M. Tayde et al., *Chin. Phys. C* **46**, 115101 (2022)
- M. Tayde, Z. Hassan, P.K. Sahoo, *Phys. Dark Universe* **42**, 101288 (2023)
- M. Tayde, J.R. Santos, J.N. Araujo, P.K. Sahoo, *Eur. Phys. J. Plus* **138**, 539 (2023)
- S. Pradhan, D. Mohanty, P.K. Sahoo, *Chin. Phys. C* **47**, 095104 (2023)
- K. Bourakadi et al., *Phys. Dark Universe* **41**, 101246 (2023)
- T.H. Loo, M. Koussour, A. De, *Ann. Phys.* **454**, 169333 (2023)
- S.A. Narawade, M. Koussour, B. Mishra, *Nucl. Phys. B* **992**, 116233 (2023)

99. J. Eiesland, *Trans. Am. Math. Soc.* **27**, 213 (1925)
100. S.K. Maurya et al., *Eur. Phys. J. C* **76**, 266 (2016)
101. D. Deb et al., *J. Cosmol. Astropart. Phys.* **2019**, 070 (2019)
102. M.K. Abubekero et al., *Astron. Rep.* **52**, 379 (2008)
103. F. Ozel, T. Guver, D. Psaltis, *Astrophys. J.* **693**, 1775 (2009)
104. P. Elebert et al., *Mon. Not. R. Astron. Soc.* **395**, 884 (2009)
105. F. Ozel, T. Guver, A. Cabrera-Lavers, P. Wroblewski, *Astrophys. J.* **712**, 964 (2010)
106. T. Guver et al., *Astrophys. J.* **719**, 1807 (2010)
107. P.B. Demorest, *Nature* **467**, 1081 (2010)
108. M.L. Rawls et al., *Astrophys. J.* **730**, 25 (2011)
109. P.C.C. Freire et al., *Mon. Not. R. Astron. Soc.* **412**, 2763 (2011)
110. S.K. Maurya et al., *Phys. Rev. D* **99**, 044029 (2019)
111. A.H. Buchdahl, *Phys. Rev. D* **116**, 1027 (1959)
112. B.V. Ivanov, *Phys. Rev. D* **65**, 104011 (2002)
113. R.C. Tolman, *Phys. Rev.* **55**, 364 (1939)
114. H. Abreu et al., *Class. Quantum Gravity* **24**, 4631 (2007)
115. L. Herrera, *Phys. Lett. A* **165**, 206 (1992)
116. M. Sharif, M.Z. Gul, *Fortschr. Phys.* **71**, 2200184 (2023)